

Search for the Cabibbo-suppressed decays $\Lambda_c^+ \rightarrow \Sigma^0 K^+ \pi^0$ and $\Lambda_c^+ \rightarrow \Sigma^0 K^+ \pi^+ \pi^-$ *

M. Ablikim(麦迪娜)¹, M. N. Achasov^{4,c}, P. Adlarson⁷⁶, X. C. Ai(艾小聪)⁸¹, R. Aliberti³⁵, A. Amoroso^{75A,75C}, Q. An(安琪)^{72,58,a}, Y. Bai(白羽)⁵⁷, O. Bakina³⁶, Y. Ban(班勇)^{46,h}, H.-R. Bao(包浩然)⁶⁴, V. Batzskaya^{1,44}, K. Begzsuren³², N. Berger³⁵, M. Berlowski⁴⁴, M. Bertani^{28A}, D. Bettoni^{29A}, F. Bianchi^{75A,75C}, E. Bianco^{75A,75C}, A. Bortone^{75A,75C}, I. Boyko³⁶, R. A. Briere⁵, A. Brueggemann⁶⁹, H. Cai(蔡浩)⁷⁷, M. H. Cai(蔡铭航)^{38,k,l}, X. Cai(蔡啸)^{1,58}, A. Calcaterra^{28A}, G. F. Cao(曹国富)^{1,64}, N. Cao(曹宁)^{1,64}, S. A. Cetin^{62A}, X. Y. Chai(柴新宇)^{46,h}, J. F. Chang(常劲帆)^{1,58}, G. R. Che(车国荣)⁴³, Y. Z. Che(车逾之)^{1,58,64}, G. Chelkov^{36,b}, C. Chen(陈琛)⁴³, C. H. Chen(陈春舟)⁹, Chao Chen(陈超)⁵⁵, G. Chen(陈刚)¹, H. S. Chen(陈和生)^{1,64}, H. Y. Chen(陈弘扬)²⁰, M. L. Chen(陈玛丽)^{1,58,64}, S. J. Chen(陈中见)⁴², S. L. Chen(陈思璐)⁴⁵, S. M. Chen(陈少敏)⁶¹, T. Chen(陈通)^{1,64}, X. R. Chen(陈旭荣)^{31,64}, X. T. Chen(陈肖婷)^{1,64}, Y. B. Chen(陈元柏)^{1,58}, Y. Q. Chen³⁴, Z. J. Chen(陈卓俊)^{25,i}, Z. K. Chen(陈梓康)⁵⁹, S. K. Choi¹⁰, X. Chu(初晓)^{12,g}, G. Cibinetto^{29A}, F. Cossio^{75C}, J. J. Cui(崔佳佳)⁵⁰, H. L. Dai(代洪亮)^{1,58}, J. P. Dai(代建平)⁷⁹, A. Dbeysi¹⁸, R. E. de Boer³, D. Dedovich³⁶, C. Q. Deng(邓创旗)⁷³, Z. Y. Deng(邓子艳)¹, A. Denig³⁵, I. Denysenko³⁶, M. Destefanis^{75A,75C}, F. De Mori^{75A,75C}, B. Ding(丁彪)^{67,1}, X. X. Ding(丁晓萱)^{46,h}, Y. Ding(丁逸)³⁴, Y. Ding(丁勇)⁴⁰, Y. X. Ding(丁玉鑫)³⁰, J. Dong(董静)^{1,58}, L. Y. Dong(董燎原)^{1,64}, M. Y. Dong(董明义)^{1,58,64}, X. Dong(董翔)⁷⁷, M. C. Du(杜蒙川)¹, S. X. Du(杜书先)⁸¹, Y. Y. Duan(段尧予)⁵⁵, Z. H. Duan(段宗欢)⁴², P. Egorov^{36,b}, G. F. Fan(樊高峰)⁴², J. J. Fan(樊俊杰)¹⁹, Y. H. Fan(范宇晗)⁴⁵, J. Fang(方进)⁵⁹, J. Fang(方建)^{1,58}, S. S. Fang(房双世)^{1,64}, W. X. Fang(方文兴)¹, Y. Q. Fang(方业泉)^{1,58}, R. Farinelli^{29A}, L. Fava^{75B,75C}, F. Feldbauer³, G. Felici^{28A}, C. Q. Feng(封常青)^{72,58}, J. H. Feng(冯俊华)⁵⁹, Y. T. Feng(冯潼)^{72,58}, M. Fritsch³, C. D. Fu(傅成栋)¹, J. L. Fu(傅金林)⁶⁴, Y. W. Fu(傅亦威)^{1,64}, H. Gao(高涵)⁶⁴, X. B. Gao(高鑫博)⁴¹, Y. N. Gao(高语浓)¹⁹, Y. N. Gao(高原宁)^{46,h}, Y. Y. Gao(高洋洋)³⁰, Yang Gao(高扬)^{72,58}, S. Garbolino^{75C}, I. Garzia^{29A,29B}, P. T. Ge(葛潘婷)¹⁹, Z. W. Ge(葛振武)⁴², C. Geng(耿聪)⁵⁹, E. M. Gersabeck⁶⁸, A. Gilman⁷⁰, K. Goetzen¹³, L. Gong(龚丽)⁴⁰, W. X. Gong(龚文煊)^{1,58}, W. Gradl³⁵, S. Gramigna^{29A,29B}, M. Greco^{75A,75C}, M. H. Gu(顾皓)^{1,58}, Y. T. Gu(顾运斤)¹⁵, C. Y. Guan(关春懿)^{1,64}, A. Q. Guo(郭爱强)³¹, L. B. Guo(郭立波)⁴¹, M. J. Guo(国梦娇)⁵⁰, R. P. Guo(郭如盼)⁴⁹, Y. P. Guo(郭玉萍)^{12,g}, A. Guskov^{36,b}, J. Gutierrez²⁷, K. L. Han(韩坤霖)⁶⁴, T. T. Han(韩婷婷)¹, F. Hanisch³, K. D. Hao(郝科迪)^{72,58}, X. Q. Hao(郝喜庆)¹⁹, F. A. Harris⁶⁶, K. K. He(何凯凯)⁵⁵, K. L. He(何康林)^{1,64}, F. H. Heinsius³, C. H. Heinz³⁵, Y. K. Heng(衡月昆)^{1,58,64}, C. Herold⁶⁰, T. Holtmann³, P. C. Hong(洪鹏程)³⁴, G. Y. Hou(侯国一)^{1,64}, X. T. Hou(侯贤涛)^{1,64}, Y. R. Hou(侯颖锐)⁶⁴, Z. L. Hou(侯治龙)¹, B. Y. Hu(胡碧颖)⁵⁹, H. M. Hu(胡海明)^{1,64}, J. F. Hu(胡继峰)^{56,j}, Q. P. Hu(胡启鹏)^{72,58}, S. L. Hu(胡圣亮)^{12,g}, T. Hu(胡涛)^{1,58,64}, Y. Hu(胡誉)¹, Z. M. Hu(胡忠敏)⁵⁹, G. S. Huang(黄光顺)^{72,58}, K. X. Huang(黄凯旋)⁵⁹, L. Q. Huang(黄麟钦)^{31,64}, P. Huang(黄盼)⁴², X. T. Huang(黄性涛)⁵⁰, Y. P. Huang(黄燕萍)¹, Y. S. Huang(黄永盛)⁵⁹, T. Hussain⁷⁴, N. Hüsken³⁵, N. in der Wiesche⁶⁹, J. Jackson²⁷, S. Janchiv³², Q. Ji(纪全)¹, Q. P. Ji(姬清平)¹⁹, W. Ji(李旺)^{1,64}, X. B. Ji(季晓斌)^{1,64}, X. L. Ji(季筱璐)^{1,58}, Y. Y. Ji(吉钰瑶)⁵⁰, Z. K. Jia(贾泽坤)^{72,58}, D. Jiang(姜地)^{1,64}, H. B. Jiang(姜候兵)⁷⁷, P. C. Jiang(蒋沛成)^{46,h}, S. J. Jiang(蒋思婧)⁹, T. J. Jiang(蒋庭俊)¹⁶, X. S. Jiang(江晓山)^{1,58,64}, Y. Jiang(蒋艺)⁶⁴, J. B. Jiao(焦健斌)⁵⁰, J. K. Jiao(焦俊坤)³⁴, Z. Jiao(焦铮)²³, S. Jin(金山)⁴², Y. Jin(金毅)⁶⁷, M. Q. Jing(荆茂强)^{1,64}, X. M. Jing(景新媚)⁶⁴, T. Johansson⁷⁶, S. Kabana³³, N. Kalantar-Nayestanaki⁶⁵, X. L. Kang(康晓琳)⁹,

Received xxxx October xxxx

* The BESIII Collaboration thanks the staff of BEPCII and the IHEP computing center for their strong support. This work is supported in part by National Key R&D Program of China under Contracts Nos. 2020YFA0406300, 2020YFA0406400, 2023YFA1606000; National Natural Science Foundation of China (NSFC) under Contracts Nos. 12205141, 11635010, 11735014, 11935015, 11935016, 11935018, 12025502, 12035009, 12035013, 12061131003, 12192260, 12192261, 12192262, 12192263, 12192264, 12192265, 12221005, 12225509, 12235017, 12361141819; Natural Science Foundation of Hunan Province (Contracts No.2024JJ2044); the Chinese Academy of Sciences (CAS) Large-Scale Scientific Facility Program; the CAS Center for Excellence in Particle Physics (CCEPP); Joint Large-Scale Scientific Facility Funds of the NSFC and CAS under Contract No. U1832207; 100 Talents Program of CAS; The Institute of Nuclear and Particle Physics (INPAC) and Shanghai Key Laboratory for Particle Physics and Cosmology; German Research Foundation DFG under Contract No. FOR5327; Istituto Nazionale di Fisica Nucleare, Italy; Knut and Alice Wallenberg Foundation under Contracts Nos. 2021.0174, 2021.0299; Ministry of Development of Turkey under Contract No. DPT2006K-120470; National Research Foundation of Korea under Contract No. NRF-2022R1A2C1092335; National Science and Technology fund of Mongolia; National Science Research and Innovation Fund (NSRF) via the Program Management Unit for Human Resources & Institutional Development, Research and Innovation of Thailand under Contracts Nos. B16F640076, B50G670107; Polish National Science Centre under Contract No. 2019/35/O/ST2/02907; Swedish Research Council under Contract No. 2019.04595; The Swedish Foundation for International Cooperation in Research and Higher Education under Contract No. CH2018-7756; U. S. Department of Energy under Contract No. DE-FG02-05ER41374.

X. S. Kang(康晓)⁴⁰, M. Kavatsyuk⁶⁵, B. C. Ke(柯百谦)⁸¹, V. Khachatryan²⁷, A. Khoukaz⁶⁹, R. Kiuchi¹, O. B. Kolcu^{62A}, B. Kopf³, M. Kuessner³, X. Kui(奎贤)^{1,64}, N. Kumar²⁶, A. Kupsc^{44,76}, W. Kühn³⁷, Q. Lan(兰强)⁷³, W. N. Lan(兰文宁)¹⁹, T. T. Lei(雷天天)^{72,58}, Z. H. Lei(雷祚弘)^{72,58}, M. Lellmann³⁵, T. Lenz³⁵, C. Li(李翠)⁴⁷, C. Li(李聪)⁴³, C. H. Li(李春花)³⁹, C. K. Li(李春凯)²⁰, Cheng Li(李澄)^{72,58}, D. M. Li(李德民)⁸¹, F. Li(李飞)^{1,58}, G. Li(李刚)¹, H. B. Li(李海波)^{1,64}, H. J. Li(李惠静)¹⁹, H. N. Li(李衡讷)^{56,j}, Hui Li(李慧)⁴³, J. R. Li(李嘉荣)⁶¹, J. S. Li(李静舒)⁵⁹, K. Li(李科)¹, K. L. Li(李凯璐)¹⁹, K. L. Li(李凯璐)^{38,k,l}, L. J. Li(李林健)^{1,64}, Lei Li(李蕾)⁴⁸, M. H. Li(李明浩)⁴³, M. R. Li(李明润)^{1,64}, P. L. Li(李佩莲)⁶⁴, P. R. Li(李培荣)^{38,k,l}, Q. M. Li(李启铭)^{1,64}, Q. X. Li(李起鑫)⁵⁰, R. Li(李燃)^{17,31}, T. Li(李腾)⁵⁰, T. Y. Li(李天佑)⁴³, W. D. Li(李卫东)^{1,64}, W. G. Li(李卫国)^{1,a}, X. Li(李旭)^{1,64}, X. H. Li(李旭红)^{72,58}, X. L. Li(李晓玲)⁵⁰, X. Y. Li(李晓宇)^{1,8}, X. Z. Li(李绪泽)⁵⁹, Y. Li(李洋)¹⁹, Y. G. Li(李彦谷)^{46,h}, Z. J. Li(李志军)⁵⁹, Z. Y. Li(李紫阳)⁷⁹, C. Liang(梁畅)⁴², H. Liang(梁昊)^{72,58}, Y. F. Liang(梁勇飞)⁵⁴, Y. T. Liang(梁羽铁)^{31,64}, G. R. Liao(廖广睿)¹⁴, L. B. Liao(廖立波)⁵⁹, M. H. Liao(廖明华)⁵⁹, Y. P. Liao(廖一朴)^{1,64}, J. Libby²⁶, A. Limphirat⁶⁰, C. C. Lin(蔺长城)⁵⁵, C. X. Lin(林创新)⁶⁴, D. X. Lin(林德旭)^{31,64}, L. Q. Lin(邵麟筌)³⁹, T. Lin(林韬)¹, B. J. Liu(刘北江)¹, B. X. Liu(刘宝鑫)⁷⁷, C. Liu(刘成)³⁴, C. X. Liu(刘春秀)¹, F. Liu(刘芳)¹, F. H. Liu(刘福虎)⁵³, Feng Liu(刘峰)⁶, G. M. Liu(刘国明)^{56,j}, H. Liu(刘昊)^{38,k,l}, H. B. Liu(刘宏邦)¹⁵, H. H. Liu(刘欢欢)¹, H. M. Liu(刘怀民)^{1,64}, Huihui Liu(刘汇慧)²¹, J. B. Liu(刘建北)^{72,58}, J. J. Liu(刘佳佳)²⁰, K. Liu(刘凯)^{38,k,l}, K. Liu(刘坤)⁷³, K. Y. Liu(刘魁勇)⁴⁰, Ke Liu(刘珂)²², L. Liu(刘亮)^{72,58}, L. C. Liu(刘良辰)⁴³, Lu Liu(刘露)⁴³, M. H. Liu(刘美宏)^{12,g}, P. L. Liu(刘佩莲)¹, Q. Liu(刘倩)⁶⁴, S. B. Liu(刘树彬)^{72,58}, T. Liu(刘桐)^{12,g}, W. K. Liu(刘维克)⁴³, W. M. Liu(刘卫民)^{72,58}, W. T. Liu(刘婉婷)³⁹, X. Liu(刘鑫)³⁹, X. Liu(刘翔)^{38,k,l}, X. Y. Liu(刘雪吟)⁷⁷, Y. Liu(刘媛)⁸¹, Y. Liu(刘义)⁸¹, Y. Liu(刘英)^{38,k,l}, Y. B. Liu(刘玉斌)⁴³, Z. A. Liu(刘振安)^{1,58,64}, Z. D. Liu(刘宗德)⁹, Z. Q. Liu(刘智青)⁵⁰, X. C. Lou(娄辛丑)^{1,58,64}, F. X. Lu(卢飞翔)⁵⁹, H. J. Lu(吕海江)²³, J. G. Lu(吕军光)^{1,58}, Y. Lu(卢宇)⁷, Y. H. Lu(卢决宏)^{1,64}, Y. P. Lu(卢云鹏)^{1,58}, Z. H. Lu(卢泽辉)^{1,64}, C. L. Luo(罗成林)⁴¹, J. R. Luo(罗家瑞)⁵⁹, J. S. Luo(罗家顺)^{1,64}, M. X. Luo(罗民兴)⁸⁰, T. Luo(罗涛)^{12,g}, X. L. Luo(罗小兰)^{1,58}, X. R. Lyu(吕晓睿)^{64,p}, Y. F. Lyu(吕翌丰)⁴³, Y. H. Lyu(吕云鹤)⁸¹, F. C. Ma(马凤才)⁴⁰, H. Ma(马衡)⁷⁹, H. L. Ma(马海龙)¹, J. L. Ma(马俊力)^{1,64}, L. L. Ma(马连良)⁵⁰, L. R. Ma(马立瑞)⁶⁷, Q. M. Ma(马秋梅)¹, R. Q. Ma(马润秋)^{1,64}, R. Y. Ma(马若云)¹⁹, T. Ma(马腾)^{72,58}, X. T. Ma(马晓天)^{1,64}, X. Y. Ma(马晓妍)^{1,58}, Y. M. Ma(马玉明)³¹, F. E. Maas¹⁸, I. MacKay⁷⁰, M. Maggiora^{75A,75C}, S. Malde⁷⁰, Y. J. Mao(冒亚军)^{46,h}, Z. P. Mao(毛泽普)¹, S. Marcello^{75A,75C}, Y. H. Meng(孟琰皓)⁶⁴, Z. X. Meng(孟召霞)⁶⁷, J. G. Messchendorp^{13,65}, G. Mezzadri^{29A}, H. Miao(妙晗)^{1,64}, T. J. Min(闵天觉)⁴², R. E. Mitchell²⁷, X. H. Mo(莫晓虎)^{1,58,64}, B. Moses²⁷, N. Yu. Muchnoi^{4,c}, J. Muskalla³⁵, Y. Nefedov³⁶, F. Nerling^{18,e}, L. S. Nie(聂麟苏)²⁰, I. B. Nikolaev^{4,c}, Z. Ning(宁哲)^{1,58}, S. Nisar^{11,m}, Q. L. Niu(牛祺乐)^{38,k,l}, S. L. Olsen^{10,64}, Q. Ouyang(欧阳群)^{1,58,64}, S. Pacetti^{28B,28C}, X. Pan(潘祥)⁵⁵, Y. Pan(潘越)⁵⁷, A. Pathak¹⁰, Y. P. Pei(裴宇鹏)^{72,58}, M. Pelizaeus³, H. P. Peng(彭海平)^{72,58}, Y. Y. Peng(彭云翊)^{38,k,l}, K. Peters^{13,e}, J. L. Ping(平加伦)⁴¹, R. G. Ping(平荣刚)^{1,64}, S. Plura³⁵, V. Prasad³³, F. Z. Qi(齐法制)¹, H. R. Qi(漆红荣)⁶¹, M. Qi(祁鸣)⁴², S. Qian(钱森)^{1,58}, W. B. Qian(钱文斌)⁶⁴, C. F. Qiao(乔从丰)⁶⁴, J. H. Qiao(乔佳辉)¹⁹, J. J. Qin(秦佳佳)⁷³, J. L. Qin(覃嘉良)⁵⁵, L. Q. Qin(秦丽清)¹⁴, L. Y. Qin(秦龙宇)^{72,58}, P. B. Qin(秦鹏勃)⁷³, X. P. Qin(覃潇平)^{12,g}, X. S. Qin(秦小帅)⁵⁰, Z. H. Qin(秦中华)^{1,58}, J. F. Qiu(邱进发)¹, Z. H. Qu(屈子皓)⁷³, C. F. Redmer³⁵, A. Rivetti^{75C}, M. Rolo^{75C}, G. Rong(荣刚)^{1,64}, S. S. Rong(荣少石)^{1,64}, Ch. Rosner¹⁸, M. Q. Ruan(阮曼奇)^{1,58}, S. N. Ruan(阮氏宁)⁴³, N. Salone⁴⁴, A. Sarantsev^{36,d}, Y. Schelhaas³⁵, K. Schoenning⁷⁶, M. Scodreggio^{29A}, K. Y. Shan(尚科羽)^{12,g}, W. Shan(单葳)²⁴, X. Y. Shan(单心钰)^{72,58}, Z. J. Shang(尚子杰)^{38,k,l}, J. F. Shangguan(上官剑锋)¹⁶, L. G. Shao(邵立港)^{1,64}, M. Shao(邵明)^{72,58}, C. P. Shen(沈成平)^{12,g}, H. F. Shen(沈宏飞)^{1,8}, W. H. Shen(沈文涵)⁶⁴, X. Y. Shen(沈肖雁)^{1,64}, B. A. Shi(施伯安)⁶⁴, H. Shi(史华)^{72,58}, J. L. Shi(石家磊)^{12,g}, J. Y. Shi(石京燕)¹, S. Y. Shi(史书宇)⁷³, X. Shi(史欣)^{1,58}, H. L. Song(宋海林)^{72,58}, J. J. Song(宋娇娇)¹⁹, T. Z. Song(宋天资)⁵⁹, W. M. Song(宋维民)^{34,1}, Y. J. Song(宋宇镜)^{12,g}, Y. X. Song(宋昀轩)^{46,h,n}, S. Sosio^{75A,75C}, S. Spataro^{75A,75C}, F. Stieler³⁵, S. S. Su(苏闪闪)⁴⁰, Y. J. Su(粟杨捷)⁶⁴, G. B. Sun(孙光尧)⁷⁷, G. X. Sun(孙功星)¹, H. Sun(孙昊)⁶⁴, H. K. Sun(孙浩凯)¹, J. F. Sun(孙俊峰)¹⁹, K. Sun(孙丹)⁶¹, L. Sun(孙亮)⁷⁷, S. S. Sun(孙胜森)^{1,64}, T. Sun^{51,f}, Y. C. Sun(孙雨长)⁷⁷, Y. H. Sun(孙益华)³⁰, Y. J. Sun(孙勇杰)^{72,58}, Y. Z. Sun(孙永昭)¹, Z. Q. Sun(孙泽群)^{1,64}, Z. T. Sun(孙振田)⁵⁰, C. J. Tang(唐昌建)⁵⁴, G. Y. Tang(唐光毅)¹, J. Tang(唐健)⁵⁹, L. F. Tang(唐林发)³⁹, M. Tang(唐嘉骏)^{72,58}, Y. A. Tang(唐迎澳)⁷⁷, L. Y. Tao(陶璐燕)⁷³, M. Tat⁷⁰, J. X. Teng(滕佳秀)^{72,58}, V. Thoren⁷⁶, J. Y. Tian(田济源)^{72,58}, W. H. Tian(田文辉)⁵⁹, Y. Tian(田野)³¹, Z. F. Tian(田飞)⁷⁷, I. Uman^{62B}, B. Wang(王斌)¹, B. Wang(王博)⁵⁹, Bo Wang(王博)^{72,58}, C. Wang(王超)¹⁹, D. Y. Wang(王大勇)^{46,h}, H. J. Wang(王泓鉴)^{38,k,l}, J. J. Wang(王家驹)⁷⁷, K. Wang(王科)^{1,58}, L. L. Wang(王亮亮)¹, L. W. Wang(王璐仪)³⁴, M. Wang(王萌)⁵⁰, M. Wang^{72,58}, N. Y. Wang(王南洋)⁶⁴, S. Wang(王石)^{38,k,l}, S. Wang(王顺)^{12,g}, T. Wang(王婷)^{12,g}, T. J. Wang(王腾蛟)⁴³, W. Wang(王维)⁷³, W. Wang(王为)⁵⁹, W. P. Wang(王维平)^{35,58,72,o}, X. Wang(王轩)^{46,h}, X. F. Wang(王雄飞)^{38,k,l}, X. J. Wang(王希俊)³⁹, X. L. Wang(王小龙)^{12,g}, X. N. Wang(王新南)¹, Y. Wang(王亦)⁶¹, Y. D. Wang(王雅迪)⁴⁵, Y. F. Wang(王贻芳)^{1,58,64}, Y. H. Wang(王英豪)^{38,k,l}, Y. L. Wang(王艺龙)¹⁹, Y. N. Wang(王燕宁)⁷⁷, Y. Q. Wang(王雨晴)¹, Yaqian Wang(王亚乾)¹⁷, Yi Wang(王义)⁶¹, Yuan Wang(王源)^{17,31}, Z. Wang(王铮)^{1,58}, Z. L. Wang(王治浪)⁷³, Z. Y. Wang(王至勇)^{1,64}, D. H. Wei(魏代会)¹⁴, F. Weidner⁶⁹, S. P. Wen(文硕频)¹, Y. R. Wen(温亚冉)³⁹, U. Wiedner³, G. Wilkinson⁷⁰, M. Wolke⁷⁶, C. Wu(吴晨)³⁹, J. F. Wu(吴金飞)^{1,8}, L. H. Wu(伍灵慧)¹, L. J. Wu(吴连近)^{1,64}, Lianjie Wu(武廉杰)¹⁹, S. G. Wu(吴韶光)^{1,64}, S. M. Wu(吴蜀明)⁶⁴, X. Wu(吴潇)^{12,g},

X. H. Wu(伍雄浩)³⁴, Y. J. Wu(吴英杰)³¹, Z. Wu(吴智)^{1,58}, L. Xia(夏磊)^{72,58}, X. M. Xian(咸秀梅)³⁹, B. H. Xiang(向本后)^{1,64}, T. Xiang(相腾)^{46,h}, D. Xiao(肖栋)^{38,k,l}, G. Y. Xiao(肖光延)⁴², H. Xiao(肖浩)⁷³, Y. L. Xiao(肖云龙)^{12,g}, Z. J. Xiao(肖振军)⁴¹, C. Xie(谢陈)⁴², K. J. Xie(谢凯吉)^{1,64}, X. H. Xie(谢昕海)^{46,h}, Y. Xie(谢勇)⁵⁰, Y. G. Xie(谢宇广)^{1,58}, Y. H. Xie(谢跃红)⁶, Z. P. Xie(谢智鹏)^{72,58}, T. Y. Xing(邢天宇)^{1,64}, C. F. Xu^{1,64}, C. J. Xu(许创杰)⁵⁹, G. F. Xu(许国发)¹, M. Xu(徐明)^{72,58}, Q. J. Xu(徐庆君)¹⁶, Q. N. Xu³⁰, W. L. Xu(徐万伦)⁶⁷, X. P. Xu(徐新平)⁵⁵, Y. Xu(徐月)⁴⁰, Y. C. Xu(胥英超)⁷⁸, Z. S. Xu(许昭)⁶⁴, F. Yan(严芳)^{12,g}, H. Y. Yan(闫浩宇)³⁹, L. Yan(严亮)^{12,g}, W. B. Yan(鄢文标)^{72,58}, W. C. Yan(闫文成)⁸¹, W. P. Yan(闫文鹏)¹⁹, X. Q. Yan(严薛强)^{1,64}, H. J. Yang(杨海军)^{51,f}, H. L. Yang(杨昊霖)³⁴, H. X. Yang(杨洪勋)¹, J. H. Yang(杨君辉)⁴², R. J. Yang(杨润佳)¹⁹, T. Yang(杨涛)¹, Y. Yang(杨莹)^{12,g}, Y. F. Yang(杨艳芳)⁴³, Y. Q. Yang(杨永强)⁹, Y. X. Yang(杨逸翔)^{1,64}, Y. Z. Yang(杨颖)¹⁹, M. Ye(叶梅)^{1,58}, M. H. Ye(叶铭汉)⁸, Junhao Yin(殷俊昊)⁴³, Z. Y. You(尤郑昀)⁵⁹, B. X. Yu(俞伯祥)^{1,58,64}, C. X. Yu(喻纯旭)⁴³, G. Yu¹³, J. S. Yu(俞洁晟)^{25,i}, M. C. Yu⁴⁰, T. Yu(于涛)⁷³, X. D. Yu(余旭东)^{46,h}, Y. C. Yu(郁烨淳)⁸¹, C. Z. Yuan(苑长征)^{1,64}, H. Yuan(袁昊)^{1,64}, J. Yuan(袁菁)³⁴, J. Yuan(袁杰)⁴⁵, L. Yuan(袁丽)², S. C. Yuan(苑思成)^{1,64}, Y. Yuan(袁野)^{1,64}, Z. Y. Yuan(袁朝阳)⁵⁹, C. X. Yue(岳崇兴)³⁹, Ying Yue(岳颖)¹⁹, A. A. Zafar⁷⁴, S. H. Zeng^{63A,63B,63C,63D}, X. Zeng(曾鑫)^{12,g}, Y. Zeng(曾云)^{25,i}, Y. J. Zeng(曾宇杰)⁵⁹, Y. J. Zeng(曾溢嘉)^{1,64}, X. Y. Zhai(翟星晔)³⁴, Y. H. Zhan(詹永华)⁵⁹, A. Q. Zhang(张安庆)^{1,64}, B. L. Zhang(张伯伦)^{1,64}, B. X. Zhang(张丙新)¹, D. H. Zhang(张丹昊)⁴³, G. Y. Zhang(张广义)¹⁹, G. Y. Zhang(张耕源)^{1,64}, H. Zhang(张豪)^{72,58}, H. Zhang(张晗)⁸¹, H. C. Zhang(张航畅)^{1,58,64}, H. H. Zhang(张宏浩)⁵⁹, H. Q. Zhang(张华桥)^{1,58,64}, H. R. Zhang(张浩然)^{72,58}, H. Y. Zhang(章红宇)^{1,58}, J. Zhang(张晋)⁵⁹, J. Zhang(张进)⁸¹, J. J. Zhang(张进军)⁵², J. L. Zhang(张杰磊)²⁰, J. Q. Zhang(张敬庆)⁴¹, J. S. Zhang(张家声)^{12,g}, J. W. Zhang(张家文)^{1,58,64}, J. X. Zhang(张景旭)^{38,k,l}, J. Y. Zhang(张建勇)¹, J. Z. Zhang(张景芝)^{1,64}, Jianyu Zhang(张剑宇)⁶⁴, L. M. Zhang(张黎明)⁶¹, Lei Zhang(张雷)⁴², N. Zhang(张楠)⁸¹, P. Zhang(张鹏)^{1,64}, Q. Zhang(张强)¹⁹, Q. Y. Zhang(张秋岩)³⁴, R. Y. Zhang(张若愚)^{38,k,l}, S. H. Zhang(张水涵)^{1,64}, Shulei Zhang(张书磊)^{25,i}, X. M. Zhang(张晓梅)¹, X. Y. Zhang⁴⁰, X. Y. Zhang(张学尧)⁵⁰, Y. Zhang(张瑶)¹, Y. Zhang(张宇)⁷³, Y. T. Zhang(张亚腾)⁸¹, Y. H. Zhang(张银鸿)^{1,58}, Y. M. Zhang(张悦明)³⁹, Z. D. Zhang(张正德)¹, Z. H. Zhang(张泽恒)¹, Z. L. Zhang(张志龙)⁵⁵, Z. L. Zhang(张兆领)³⁴, Z. X. Zhang(张泽祥)¹⁹, Z. Y. Zhang(张振宇)⁷⁷, Z. Y. Zhang(张子羽)⁴³, Z. Z. Zhang(张子扬)⁴⁵, Zh. Zh. Zhang¹⁹, G. Zhao(赵光)¹, J. Y. Zhao(赵静宜)^{1,64}, J. Z. Zhao(赵京周)^{1,58}, L. Zhao(赵玲)¹, Lei Zhao(赵雷)^{72,58}, M. G. Zhao(赵明刚)⁴³, N. Zhao(赵宁)⁷⁹, R. P. Zhao(赵若平)⁶⁴, S. J. Zhao(赵书俊)⁸¹, Y. B. Zhao(赵豫斌)^{1,58}, Y. L. Zhao(赵艳琳)⁵⁵, Y. X. Zhao(赵宇翔)^{31,64}, Z. G. Zhao(赵政国)^{72,58}, A. Zhemchugov^{36,b}, B. Zheng(郑波)⁷³, B. M. Zheng(郑变敏)³⁴, J. P. Zheng(郑建平)^{1,58}, W. J. Zheng(郑文静)^{1,64}, X. R. Zheng(郑心如)¹⁹, Y. H. Zheng(郑阳恒)^{64,p}, B. Zhong(钟彬)⁴¹, X. Zhong(钟鑫)⁵⁹, H. Zhou(周航)^{35,50,o}, J. Y. Zhou(周佳莹)³⁴, S. Zhou(周帅)⁶, X. Zhou(周详)⁷⁷, X. K. Zhou(周晓康)⁶, X. R. Zhou(周小蓉)^{72,58}, X. Y. Zhou(周兴玉)³⁹, Y. Z. Zhou(周卓)^{12,g}, Z. C. Zhou(周章丞)²⁰, A. N. Zhu(朱傲男)⁶⁴, J. Zhu(朱江)⁴³, K. Zhu(朱凯)¹, K. J. Zhu(朱科军)^{1,58,64}, K. S. Zhu(朱康帅)^{12,g}, L. Zhu(朱林)³⁴, L. X. Zhu(朱琳莹)⁶⁴, S. H. Zhu(朱世海)⁷¹, T. J. Zhu(朱腾蛟)^{12,g}, W. D. Zhu(朱稳定)⁴¹, W. J. Zhu(朱文静)¹, W. Z. Zhu(朱文卓)¹⁹, Y. C. Zhu(朱莹春)^{72,58}, Z. A. Zhu(朱自安)^{1,64}, X. Y. Zhuang(庄新宇)⁴³, J. H. Zou(邹佳恒)¹, J. Zu(祖健)^{72,58}

(BESIII Collaboration)

¹ Institute of High Energy Physics, Beijing 100049, People's Republic of China

² Beihang University, Beijing 100191, People's Republic of China

³ Bochum Ruhr-University, D-44780 Bochum, Germany

⁴ Budker Institute of Nuclear Physics SB RAS (BINP), Novosibirsk 630090, Russia

⁵ Carnegie Mellon University, Pittsburgh, Pennsylvania 15213, USA

⁶ Central China Normal University, Wuhan 430079, People's Republic of China

⁷ Central South University, Changsha 410083, People's Republic of China

⁸ China Center of Advanced Science and Technology, Beijing 100190, People's Republic of China

⁹ China University of Geosciences, Wuhan 430074, People's Republic of China

¹⁰ Chung-Ang University, Seoul, 06974, Republic of Korea

¹¹ COMSATS University Islamabad, Lahore Campus, Defence Road, Off Raiwind Road, 54000 Lahore, Pakistan

¹² Fudan University, Shanghai 200433, People's Republic of China

¹³ GSI Helmholtzcentre for Heavy Ion Research GmbH, D-64291 Darmstadt, Germany

¹⁴ Guangxi Normal University, Guilin 541004, People's Republic of China

¹⁵ Guangxi University, Nanning 530004, People's Republic of China

¹⁶ Hangzhou Normal University, Hangzhou 310036, People's Republic of China

¹⁷ Hebei University, Baoding 071002, People's Republic of China

¹⁸ Helmholtz Institute Mainz, Staudinger Weg 18, D-55099 Mainz, Germany

¹⁹ Henan Normal University, Xinxiang 453007, People's Republic of China

²⁰ Henan University, Kaifeng 475004, People's Republic of China

²¹ Henan University of Science and Technology, Luoyang 471003, People's Republic of China

²² Henan University of Technology, Zhengzhou 450001, People's Republic of China

- ²³ Huangshan College, Huangshan 245000, People's Republic of China
- ²⁴ Hunan Normal University, Changsha 410081, People's Republic of China
- ²⁵ Hunan University, Changsha 410082, People's Republic of China
- ²⁶ Indian Institute of Technology Madras, Chennai 600036, India
- ²⁷ Indiana University, Bloomington, Indiana 47405, USA
- ²⁸ INFN Laboratori Nazionali di Frascati, (A)INFN Laboratori Nazionali di Frascati, I-00044, Frascati, Italy; (B)INFN Sezione di Perugia, I-06100, Perugia, Italy; (C)University of Perugia, I-06100, Perugia, Italy
- ²⁹ INFN Sezione di Ferrara, (A)INFN Sezione di Ferrara, I-44122, Ferrara, Italy; (B)University of Ferrara, I-44122, Ferrara, Italy
- ³⁰ Inner Mongolia University, Hohhot 010021, People's Republic of China
- ³¹ Institute of Modern Physics, Lanzhou 730000, People's Republic of China
- ³² Institute of Physics and Technology, Peace Avenue 54B, Ulaanbaatar 13330, Mongolia
- ³³ Instituto de Alta Investigación, Universidad de Tarapacá, Casilla 7D, Arica 1000000, Chile
- ³⁴ Jilin University, Changchun 130012, People's Republic of China
- ³⁵ Johannes Gutenberg University of Mainz, Johann-Joachim-Becher-Weg 45, D-55099 Mainz, Germany
- ³⁶ Joint Institute for Nuclear Research, 141980 Dubna, Moscow region, Russia
- ³⁷ Justus-Liebig-Universität Giessen, II. Physikalisches Institut, Heinrich-Buff-Ring 16, D-35392 Giessen, Germany
- ³⁸ Lanzhou University, Lanzhou 730000, People's Republic of China
- ³⁹ Liaoning Normal University, Dalian 116029, People's Republic of China
- ⁴⁰ Liaoning University, Shenyang 110036, People's Republic of China
- ⁴¹ Nanjing Normal University, Nanjing 210023, People's Republic of China
- ⁴² Nanjing University, Nanjing 210093, People's Republic of China
- ⁴³ Nankai University, Tianjin 300071, People's Republic of China
- ⁴⁴ National Centre for Nuclear Research, Warsaw 02-093, Poland
- ⁴⁵ North China Electric Power University, Beijing 102206, People's Republic of China
- ⁴⁶ Peking University, Beijing 100871, People's Republic of China
- ⁴⁷ Qufu Normal University, Qufu 273165, People's Republic of China
- ⁴⁸ Renmin University of China, Beijing 100872, People's Republic of China
- ⁴⁹ Shandong Normal University, Jinan 250014, People's Republic of China
- ⁵⁰ Shandong University, Jinan 250100, People's Republic of China
- ⁵¹ Shanghai Jiao Tong University, Shanghai 200240, People's Republic of China
- ⁵² Shanxi Normal University, Linfen 041004, People's Republic of China
- ⁵³ Shanxi University, Taiyuan 030006, People's Republic of China
- ⁵⁴ Sichuan University, Chengdu 610064, People's Republic of China
- ⁵⁵ Soochow University, Suzhou 215006, People's Republic of China
- ⁵⁶ South China Normal University, Guangzhou 510006, People's Republic of China
- ⁵⁷ Southeast University, Nanjing 211100, People's Republic of China
- ⁵⁸ State Key Laboratory of Particle Detection and Electronics, Beijing 100049, Hefei 230026, People's Republic of China
- ⁵⁹ Sun Yat-Sen University, Guangzhou 510275, People's Republic of China
- ⁶⁰ Suranaree University of Technology, University Avenue 111, Nakhon Ratchasima 30000, Thailand
- ⁶¹ Tsinghua University, Beijing 100084, People's Republic of China
- ⁶² Turkish Accelerator Center Particle Factory Group, (A)Istinye University, 34010, Istanbul, Turkey; (B)Near East University, Nicosia, North Cyprus, 99138, Mersin 10, Turkey
- ⁶³ University of Bristol, H H Wills Physics Laboratory, Tyndall Avenue, Bristol, BS8 1TL, UK
- ⁶⁴ University of Chinese Academy of Sciences, Beijing 100049, People's Republic of China
- ⁶⁵ University of Groningen, NL-9747 AA Groningen, The Netherlands
- ⁶⁶ University of Hawaii, Honolulu, Hawaii 96822, USA
- ⁶⁷ University of Jinan, Jinan 250022, People's Republic of China
- ⁶⁸ University of Manchester, Oxford Road, Manchester, M13 9PL, United Kingdom
- ⁶⁹ University of Muenster, Wilhelm-Klemm-Strasse 9, 48149 Muenster, Germany
- ⁷⁰ University of Oxford, Keble Road, Oxford OX13RH, United Kingdom
- ⁷¹ University of Science and Technology Liaoning, Anshan 114051, People's Republic of China
- ⁷² University of Science and Technology of China, Hefei 230026, People's Republic of China
- ⁷³ University of South China, Hengyang 421001, People's Republic of China
- ⁷⁴ University of the Punjab, Lahore-54590, Pakistan
- ⁷⁵ University of Turin and INFN, (A)University of Turin, I-10125, Turin, Italy; (B)University of Eastern Piedmont, 010201-4

I-15121, Alessandria, Italy; (C)INFN, I-10125, Turin, Italy

⁷⁶ Uppsala University, Box 516, SE-75120 Uppsala, Sweden

⁷⁷ Wuhan University, Wuhan 430072, People's Republic of China

⁷⁸ Yantai University, Yantai 264005, People's Republic of China

⁷⁹ Yunnan University, Kunming 650500, People's Republic of China

⁸⁰ Zhejiang University, Hangzhou 310027, People's Republic of China

⁸¹ Zhengzhou University, Zhengzhou 450001, People's Republic of China

^a Deceased

^b Also at the Moscow Institute of Physics and Technology, Moscow 141700, Russia

^c Also at the Novosibirsk State University, Novosibirsk, 630090, Russia

^d Also at the NRC "Kurchatov Institute", PNPI, 188300, Gatchina, Russia

^e Also at Goethe University Frankfurt, 60323 Frankfurt am Main, Germany

^f Also at Key Laboratory for Particle Physics, Astrophysics and Cosmology, Ministry of Education; Shanghai Key Laboratory for Particle Physics and Cosmology; Institute of Nuclear and Particle Physics, Shanghai 200240, People's Republic of China

^g Also at Key Laboratory of Nuclear Physics and Ion-beam Application (MOE) and Institute of Modern Physics, Fudan University, Shanghai 200443, People's Republic of China

^h Also at State Key Laboratory of Nuclear Physics and Technology, Peking University, Beijing 100871, People's Republic of China

ⁱ Also at School of Physics and Electronics, Hunan University, Changsha 410082, China

^j Also at Guangdong Provincial Key Laboratory of Nuclear Science, Institute of Quantum Matter, South China Normal University, Guangzhou 510006, China

^k Also at MOE Frontiers Science Center for Rare Isotopes, Lanzhou University, Lanzhou 730000, People's Republic of China

^l Also at Lanzhou Center for Theoretical Physics, Lanzhou University, Lanzhou 730000, People's Republic of China

^m Also at the Department of Mathematical Sciences, IBA, Karachi 75270, Pakistan

ⁿ Also at Ecole Polytechnique Federale de Lausanne (EPFL), CH-1015 Lausanne, Switzerland

^o Also at Helmholtz Institute Mainz, Staudinger Weg 18, D-55099 Mainz, Germany

^p Also at Hangzhou Institute for Advanced Study, University of Chinese Academy of Sciences, Hangzhou 310024, China

Abstract

Utilizing 4.5 fb^{-1} of e^+e^- annihilation data collected at center-of-mass energies ranging from 4599.53 MeV to 4698.82 MeV by the BESIII detector at the BEPCII collider, we search for the singly Cabibbo-suppressed hadronic decays $\Lambda_c^+ \rightarrow \Sigma^0 K^+ \pi^0$ and $\Lambda_c^+ \rightarrow \Sigma^0 K^+ \pi^+ \pi^-$ with a single-tag method. No significant signals are observed for both decays. The upper limits on the branching fractions at the 90% confidence level are determined to be 5.0×10^{-4} for $\Lambda_c^+ \rightarrow \Sigma^0 K^+ \pi^0$ and 6.5×10^{-4} for $\Lambda_c^+ \rightarrow \Sigma^0 K^+ \pi^+ \pi^-$.

Key words Charmed baryon, SCS decay, BESIII Experiment

1 Introduction

The experimental investigation of the decays of charmed baryons plays a critical role in understanding the complex dynamics of strong and weak interactions involving heavy quarks. The charmed baryon, Λ_c^+ , was first observed by the Mark II experiment in 1979 [1]. However, despite the decades of research, the sum of the known Λ_c^+ decay branching fractions (BFs) is still limited to about 70%, with the remaining decays yet to be measured [2, 3]. The hadronic decay amplitudes of Λ_c^+ include both factorizable and nonfactorizable contributions. Unlike charmed meson decays, where factorizable contributions are dominant due to higher emitted energy [4],

the weak hadronic decays of Λ_c^+ are not suppressed by color or helicity [5]. As a result, they receive significant non-factorizable contributions, such as those from the W -exchange diagrams. Although extensive studies with various phenomenological models have been performed on hadronic Λ_c^+ decays, the interference between the W -emission and W -exchange amplitudes remains unclear currently. Therefore, it is essential to further improve the measurements of the BFs of Cabibbo-favored (CF) and singly Cabibbo-suppressed (SCS) decays of Λ_c^+ .

Study of the three-body hadronic decays $\Lambda_c^+ \rightarrow B_n PP'$ is an important area of research, where B_n and $P(P')$ denote octet baryon and pseudoscalar meson, respectively. To date, the SCS hadronic decay

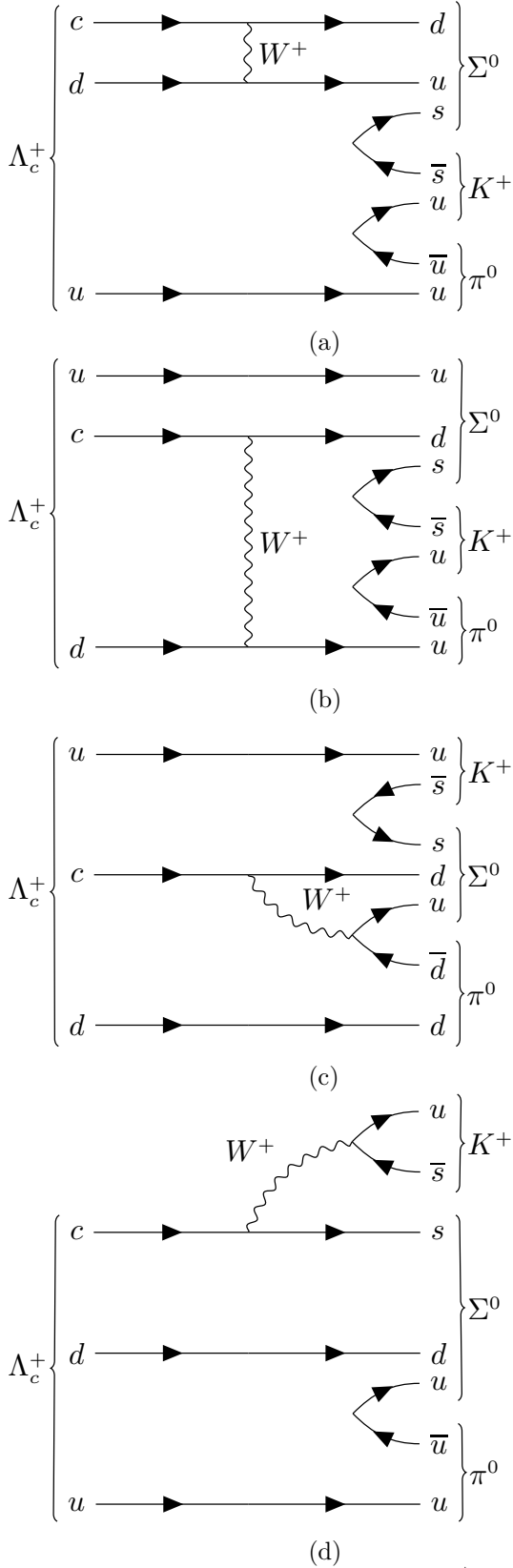


Figure 1. The Feynman diagrams of $\Lambda_c^+ \rightarrow \Sigma^0 K^+ \pi^0$: (a) and (b) W -exchange diagrams, (c) Internal W -emission diagram, and (d) External W -emission diagram.

proceed via the Feynman diagrams shown in Fig. 1. Predictions of the decay BF range from 0.8×10^{-3} to 1.2×10^{-3} with the SU(3) flavor symmetry framework [6–8], under the assumption that the PP' system is in an S -wave state. The most recent prediction, as reported in Ref. [8], considers the complete effective Hamiltonian contribution. On the other hand, Ref. [9] predicts the BF of $\Lambda_c^+ \rightarrow \Sigma^0 K^+ \pi^0$ to be $(2.1 \pm 0.6) \times 10^{-3}$ with the statistical isospin model. Experimentally, the BESIII experiment searched for this decay for the first time using a double-tag method and set an upper limit on its BF at the 90% confidence level (C.L.) to be 1.8×10^{-3} [10].

Currently, there are no theoretical predictions of the four-body hadronic decay $\Lambda_c^+ \rightarrow \Sigma^0 K^+ \pi^+ \pi^-$. The BaBar experiment performed the first search for this decay and reported an upper limit on the BF ratio $\frac{\mathcal{B}(\Lambda_c^+ \rightarrow \Sigma^0 K^+ \pi^+ \pi^-)}{\mathcal{B}(\Lambda_c^+ \rightarrow \Sigma^0 \pi^+ \pi^-)} < 2.0 \times 10^{-2}$ at the 90% C.L. [11].

In this work, we search for the hadronic decays $\Lambda_c^+ \rightarrow \Sigma^0 K^+ \pi^0$ and $\Lambda_c^+ \rightarrow \Sigma^0 K^+ \pi^+ \pi^-$, with subsequent decay $\Sigma^0 \rightarrow \gamma \Lambda$, utilizing 4.5 fb^{-1} of e^+e^- annihilation data collected at center-of-mass (c.m.) energies ranging from 4599.53 MeV to 4698.82 MeV [12–14]. Throughout this paper, the charge-conjugate state is always implied.

2 BESIII detector and Monte Carlo simulation

The BESIII detector [15] records symmetric e^+e^- collisions provided by the BEPCII storage ring [16] in the c.m. energy range from 1.84 to 4.95 GeV, with a peak luminosity of $1.1 \times 10^{33} \text{ cm}^{-2} \text{ s}^{-1}$ achieved at $\sqrt{s} = 3.773 \text{ GeV}$. BESIII has collected large data samples in this energy region [20]. The cylindrical core of the BESIII detector covers 93% of the full solid angle and consists of a helium-based multilayer drift chamber (MDC), a plastic scintillator time-of-flight system (TOF), and a CsI(Tl) electromagnetic calorimeter (EMC), which are all enclosed in a superconducting solenoidal magnet providing a 1.0 T magnetic field. The solenoid is supported by an octagonal flux-return yoke with resistive plate counter muon identification modules interleaved with steel. The charged-particle momentum resolution at 1 GeV/ c is 0.5%, and the dE/dx resolution is 6% for electrons from Bhabha scattering. The EMC measures photon energies with a resolution of 2.5% (5%) at 1 GeV in the barrel (end-cap) region. The time resolution in the TOF barrel region is 68 ps, while that in the end-cap region was 110 ps. The end-cap TOF system was upgraded in 2015 using multigap resistive plate

chamber technology, providing a time resolution of 60 ps [17–19]. About 87% of the data used in this analysis benefits from this upgrade.

Simulated samples, generated using the GEANT4-based [21] Monte Carlo (MC) package, which includes the geometric description of the BESIII detector and the detector response, are used to determine the detection efficiency and to estimate the backgrounds. The simulation includes the beam energy spread and initial state radiation (ISR) in the e^+e^- annihilation, modeled with the generator KKMC [22]. For the ISR simulation, the Born cross section line shape of $e^+e^- \rightarrow \Lambda_c^+ \bar{\Lambda}_c^-$ measured by BESIII is used [23]. Signal MC samples are generated as $\Lambda_c^+ \rightarrow \Sigma^0 K^+ \pi^0$, $\Lambda_c^+ \rightarrow \Sigma^0 \pi^+ \pi^0$, $\Lambda_c^+ \rightarrow \Sigma^0 K^+ \pi^+ \pi^-$, and $\Lambda_c^+ \rightarrow \Sigma^0 \pi^+ \pi^+ \pi^-$, with the $\bar{\Lambda}_c^-$ baryon decays inclusively. The signal decays are produced using the phase space (PHSP) model. To calculate the detection efficiencies, one million signal MC events are generated for each energy point, where Λ_c^+ ($\bar{\Lambda}_c^-$) decays into the signal mode, and $\bar{\Lambda}_c^-$ (Λ_c^+) decays into all possible states. Additionally, to study the peaking background, exclusive MC samples of $\Lambda_c^+ \rightarrow \Xi^0 K^+$ and $\Lambda_c^+ \rightarrow \Lambda K^{*+}$ are generated. Inclusive MC samples consist of open-charm states, ISR production of the J/ψ and $\psi(3686)$ states, and continuum processes $e^+e^- \rightarrow q\bar{q}$ ($q = u, d, s$) are used to study backgrounds. The known decay modes of charmed hadrons and charmonium states are modeled with EVTGEN [24, 25] using BFs taken from the Particle Data Group (PDG) [2], and the remaining unknown decays are modeled with LUNDCHARM [26, 27]. Final state radiation from charged final-state particles is incorporated with the PHOTOS package [28].

3 Event selection and data analysis

Due to limited data statistics, we adopt a single-tag approach to improve signal efficiencies, where only one Λ_c^+ is reconstructed in each event, with no requirement on the recoil side. To avoid potential bias and validate the analysis procedure, a blind analysis is adopted to analyze pseudodata, such as the inclusive MC sample with equivalent size as data. The real data is unblinded after the analysis procedure has been fixed.

All charged tracks are required to have a polar angle (θ) range within $|\cos\theta| < 0.93$, where θ is defined with respect to the z axis, which is the symmetry axis of the MDC. For the charged tracks not originating from Λ decays, the distance of closest approach to the interaction point (IP) must be less than

10 cm along the z -axis, $|V_z|$, and less than 1 cm in the transverse plane, V_{xy} . Particle identification (PID) for charged tracks combines measurements of the energy deposited in the MDC (dE/dx) and the flight time in the TOF to form likelihoods $\mathcal{L}(h)$ ($h = p, K, \pi$) for each hadron h hypothesis. Tracks are identified as protons when the proton hypothesis has the greatest likelihood ($\mathcal{L}(p) > \mathcal{L}(K)$ and $\mathcal{L}(p) > \mathcal{L}(\pi)$), while charged kaons and pions are identified by comparing the likelihoods for the kaon and pion hypotheses, $\mathcal{L}(K) > \mathcal{L}(\pi)$ and $\mathcal{L}(\pi) > \mathcal{L}(K)$, respectively.

The Λ particles are reconstructed from a pair of oppositely charged proton and pion candidates satisfying $|V_z| < 20$ cm. The same PID requirements as mentioned before are imposed to select the proton candidates. Other charged tracks are assigned to be π candidate without any PID requirements. These charged tracks are constrained to originate from the common decay vertex by requiring the χ^2 of the vertex fit to be less than 100, and the decay length is required to be greater than twice the vertex resolution away from the IP. To ensure reconstruction reliability, the Λ candidates are required to have an invariant mass within $1.111 < M(p\pi^-) < 1.121$ GeV/ c^2 , which corresponds to three times of the mass resolution around the known Λ mass [2].

Photon candidates are identified using isolated showers in the EMC. The deposited energy of each shower must be more than 25 MeV in the barrel region ($|\cos\theta| < 0.80$) and more than 50 MeV in the end cap region ($0.86 < |\cos\theta| < 0.92$). To exclude showers that originate from charged tracks, the angle subtended by the EMC shower and the position of the closest charged track at the EMC must be greater than 10° as measured from the IP. To suppress electronic noise and showers unrelated to the event, the difference between the EMC time and the event start time is required to be within $[0, 700]$ ns. The π^0 candidates are reconstructed from photon pairs with an invariant mass within $0.115 < M(\gamma\gamma) < 0.150$ GeV/ c^2 . To improve momentum resolution, a one-constraint kinematic fit is utilized to constrain the $M(\gamma\gamma)$ to the known π^0 mass [2]. Only combinations that satisfy $\chi^2 < 200$ are retained, and the refined momenta are then employed for subsequent analysis. Then, the Σ^0 candidates are reconstructed from the $\Lambda\gamma$ final states, with an invariant mass in the range $1.179 < M(\Lambda\gamma) < 1.203$ GeV/ c^2 .

To reduce the effect from the noise produced by \bar{p} in the EMC, the opening angle between photon and antiproton is required to be greater than 20° , which is obtained by optimizing the figure-of-merit defined

as $FOM = \frac{\varepsilon}{2.5 + \sqrt{B}}$ [29]. Here, ε is the signal efficiency and B denotes the background yield from the inclusive MC samples. By utilizing the generic event-type analysis tool TopoAna [30], the study of inclusive MC samples shows that the peaking backgrounds for $\Lambda_c^+ \rightarrow \Sigma^0 K^+ \pi^0$ are from the $\Lambda_c^+ \rightarrow \Xi^0 K^+$ and $\Lambda_c^+ \rightarrow \Lambda K^{*+}$ decays. These backgrounds involve one less photon in the final state than the signal process. To suppress these backgrounds, we define the energy difference $\Delta E_{p\pi^- K^+ \gamma\gamma} \equiv E_p + E_{\pi^-} + E_{K^+} + E_{\gamma 1} + E_{\gamma 2} - E_{\text{beam}}$, where E_p , E_{π^-} , E_{K^+} , and $E_{\gamma 1/2}$ are the energies of the proton, pion, kaon, and two photons, respectively while E_{beam} representing the beam energy. Candidate events for $\Lambda_c^+ \rightarrow \Sigma^0 K^+ \pi^0$ are required to satisfy $-160 < \Delta E_{p\pi^- K^+ \gamma\gamma} < -30$ MeV; while candidate events for $\Lambda_c^+ \rightarrow \Sigma^0 K^+ \pi^+ \pi^-$ are required to satisfy $\Delta E_{p\pi^- K^+ \pi^+ \pi^-} < -40$ MeV. The distributions of $\Delta E_{p\pi^- K^+ \gamma\gamma}$ ($\Delta E_{p\pi^- K^+ \pi^+ \pi^-}$) are shown in Fig. 2.

After applying the above requirements, The Σ^0 , K^+ and π^0 (π^\pm) candidates are combined to reconstruct the Λ_c^+ . Kinematic variables, including energy difference ΔE , defined as $\Delta E \equiv E_{\text{rec-}\Lambda_c^+} - E_{\text{beam}}$, and the beam-constrained mass M_{BC} , defined as $M_{\text{BC}} \equiv \sqrt{E_{\text{beam}}^2/c^4 - |\vec{p}|^2/c^2}$, are utilized to identify Λ_c^+ candidates. Here, $E_{\text{rec-}\Lambda_c^+}$ and \vec{p} are the energy and momentum of Λ_c^+ candidate, respectively. If there are multiple combinations satisfying these requirements in an event, the one with the minimum $|\Delta E|$ is retained. Candidate events for $\Lambda_c^+ \rightarrow \Sigma^0 K^+ \pi^0$ and $\Lambda_c^+ \rightarrow \Sigma^0 K^+ \pi^+ \pi^-$ are required to satisfy $\Delta E \in [-27, 6]$ MeV and $\Delta E \in [-21, 7]$ MeV respectively, with the ranges optimized according to the FOM. The signal efficiency and background yield are obtained within the M_{BC} signal region of $M_{\text{BC}} \in [2.282, 2.291]$ GeV/ c^2 . To obtain a pure signal, we have employed the truth-match method [31]. This method involves comparing two photons in the π^0 , one photon in the Σ^0 , and the charged tracks K^\pm and π^\pm with their corresponding truth information. The angle θ_{truth} is defined as the opening angle between each reconstructed tracks (showers) and its corresponding simulated tracks (showers). The signal shape is derived from events where θ_{truth} is less than 20° for all tracks (showers).

Table 1 lists the signal efficiencies obtained at different energy points. Figure 3 shows the M_{BC} distributions of the simultaneous fit performed between different energy points for each of the signal decays, where no clear Λ_c^+ signals are observed. A likelihood scan method is employed after incorporating the systematic uncertainties, as discussed in the next section, to estimate the upper limits.

The absolute BF of the signal decay is determined by

$$\mathcal{B}^{\text{sig}} \equiv \frac{N^{\text{sig}}}{2 \cdot N_{\Lambda_c^+ \Lambda_c^-} \cdot \mathcal{B}^{\text{inter}} \cdot \varepsilon^{\text{sig}}}, \quad (1)$$

where $N_{\Lambda_c^+ \Lambda_c^-}$ is the total number of $\Lambda_c^+ \bar{\Lambda}_c^-$ pairs, ε^{sig} is the single-tag efficiency, and $\mathcal{B}^{\text{inter}}$ is the product BFs of the intermediate states Σ^0 , Λ and π^0 .

Table 1. Single-tag efficiencies (%) for $\Lambda_c^+ \rightarrow \Sigma^0 K^+ \pi^0$ and $\Lambda_c^+ \rightarrow \Sigma^0 K^+ \pi^+ \pi^-$ at different energy points, where the uncertainties are statistical only.

\sqrt{s} (MeV)	$\varepsilon_{\Lambda_c^+ \rightarrow \Sigma^0 K^+ \pi^0}$	$\varepsilon_{\Lambda_c^+ \rightarrow \Sigma^0 K^+ \pi^+ \pi^-}$
4599.53	5.17±0.04	3.44±0.03
4611.86	4.89±0.03	3.10±0.03
4628.00	4.76±0.03	3.14±0.03
4640.91	4.76±0.03	3.21±0.03
4661.24	4.71±0.03	3.32±0.03
4681.92	4.68±0.03	3.43±0.03
4698.82	4.65±0.03	3.44±0.03

Since there are different distributions of background and signal events at each energy point, a simultaneous fit is performed on individual M_{BC} distributions. The BF of each signal decay is constrained to be the same value through a maximum likelihood simultaneous fit to individual M_{BC} distributions across seven energy points. In the fit, the signal shapes are derived from MC simulations convolved with Gaussian functions to account for the potential difference between data the MC simulations, due to imperfect modeling in MC simulation and the beam-energy spread. The control samples of $\Lambda_c^+ \rightarrow \Sigma^0 \pi^+ \pi^0$ and $\Lambda_c^+ \rightarrow \Sigma^0 \pi^+ \pi^+ \pi^-$ are used to evaluate the resolution, which have similar topologies as our signal decays. The combinatorial backgrounds are well described by the ARGUS function [32] with c.m. energy dependent endpoint fixed at E_{beam} . The remaining peaking backgrounds, $\Lambda_c^+ \rightarrow \Xi^0 K^+$ and $\Lambda_c^+ \rightarrow \Lambda K^{*+}$ for $\Lambda_c^+ \rightarrow \Sigma^0 K^+ \pi^0$, are described using exclusive MC simulations with yields determined by the known BFs and the simulated misidentification rates as listed in Table 2. For $\Lambda_c^+ \rightarrow \Sigma^0 K^+ \pi^+ \pi^-$, there is no significant peaking background. Unmatched events, studied through the signal MC samples, exhibit a non-flat distribution. In the simultaneous fit, the yields associated with the unmatched events are determined by evaluating the ratio between the matched signal yields and the unmatched background yields, with the ratio obtained from MC simulation.

Table 2. The contamination rates (%) after including the BFs of the secondary decays at

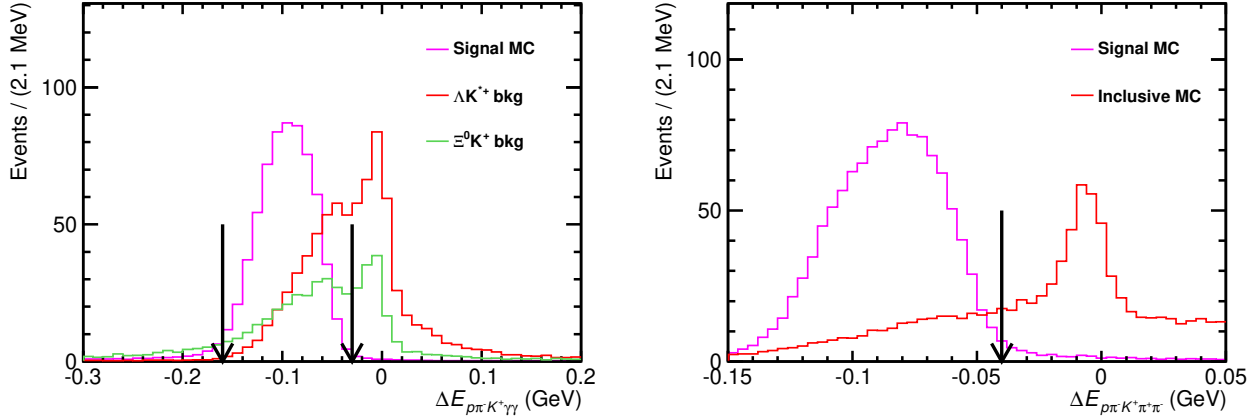


Figure 2. The distributions of $\Delta E_{p\pi^-K^+\gamma\gamma}$ ($\Delta E_{p\pi^-K^+\pi^+\pi^-}$) for $\Lambda_c^+ \rightarrow \Sigma^0 K^+ \pi^0$ ($\Lambda_c^+ \rightarrow \Sigma^0 K^+ \pi^+ \pi^-$). The histograms of the signal MC are normalized to make the distribution more intuitive when compared to the inclusive MC.

each energy point, where the uncertainties are statistical only.

\sqrt{s} (MeV)	$\epsilon_{\Lambda_c^+ \rightarrow \Xi^0 K^+}$	$\epsilon_{\Lambda_c^+ \rightarrow \Lambda K^{*+}}$
4599.53	2.34 ± 0.03	2.63 ± 0.02
4611.86	1.97 ± 0.03	2.59 ± 0.02
4628.00	2.10 ± 0.03	2.58 ± 0.02
4640.91	2.06 ± 0.03	2.58 ± 0.02
4661.24	2.10 ± 0.03	2.57 ± 0.02
4681.92	2.14 ± 0.03	2.56 ± 0.02
4698.82	2.25 ± 0.03	2.46 ± 0.02

4 Systematic uncertainty

The systematic uncertainties in the determinations of the upper limits on the BFs are classified into two categories: additive terms and multiplicative terms.

The additive terms include the uncertainties introduced by the chosen signal and background shapes. The uncertainty associated with the signal shape is estimated by changing the parameters of the convolved Gaussian functions within their uncertainties. The largest deviation of the individual changes is taken as the uncertainty. The background shape of the non-peaking components is changed from the ARGUS function to be the shape extracted from the inclusive MC samples. The uncertainty due to the fixed contribution of the peaking background yields in the fit is investigated by varying the fixed yields within $\pm 1\sigma$ of the PDG BFs of individual background sources. Among all the above terms, the case yielding the largest upper limit is chosen for further analysis. The additive uncertainty for $\Lambda_c^+ \rightarrow \Sigma^0 K^+ \pi^+ \pi^-$ is dominated by the signal shape uncertainty, while

the $\Lambda_c^+ \rightarrow \Sigma^0 K^+ \pi^0$ is mainly influenced by the background shape uncertainty.

The sources of multiplicative systematic uncertainties include tracking and PID of charged particles, π^0 reconstruction, Λ reconstruction, photon reconstruction, ΔE requirement, $\mathcal{B}^{\text{inter}}$ (Quoted BF), MC model, truth matching, MC statistics, $N_{\Lambda_c^+ \bar{\Lambda}_c^-}$, ΔE_Λ ($\Delta E_{p\pi^-K^+\gamma\gamma}$ and $\Delta E_{p\pi^-K^+\pi^+\pi^-}$) and $\theta_{\bar{p}\gamma}$ requirement. The total multiplicative systematic uncertainties are summarized in Table 3 and discussed in details below.

Table 3. Multiplicative systematic uncertainties in unit of % for the BF measurement.

Source	$\Lambda_c^+ \rightarrow \Sigma^0 K^+ \pi^0$	$\Lambda_c^+ \rightarrow \Sigma^0 K^+ \pi^+ \pi^-$
Tracking	1.0	3.0
PID	1.0	3.0
π^0 reconstruction	3.1	-
Λ reconstruction	2.5	2.5
Photon detection	0.5	0.5
ΔE requirement	2.0	3.7
MC model	5.5	18.5
$\mathcal{B}^{\text{inter}}$	0.8	0.8
Truth matching	5.5	4.9
$N_{\Lambda_c^+ \bar{\Lambda}_c^-}$	0.9	0.9
MC statistics	0.5	0.3
ΔE_Λ requirement	0.4	0.3
$\theta_{\bar{p}\gamma}$ requirement	0.1	-
Total	9.2	20.1

- Tracking and PID: The uncertainties of either PID or tracking of the charged tracks are quoted as 1.0% per track based on studies of the control sample of $e^+e^- \rightarrow K^+K^-\pi^+\pi^-$ [33].
- π^0 reconstruction: The π^0 reconstruction efficiency is studied with the control samples of

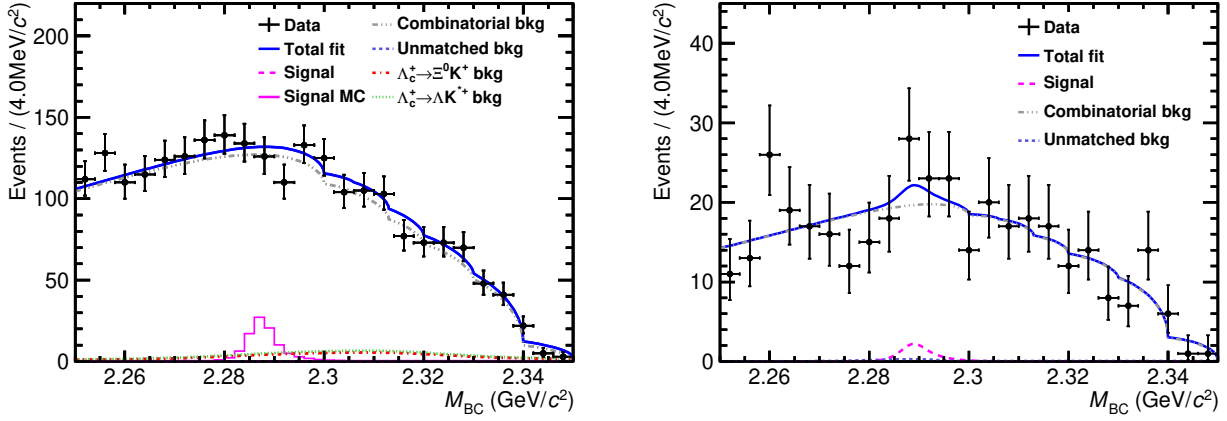


Figure 3. The fit to the M_{BC} distributions of $\Lambda_c^+ \rightarrow \Sigma^0 K^+ \pi^0$ (left) and $\Lambda_c^+ \rightarrow \Sigma^0 K^+ \pi^+ \pi^-$ (right) of the combined data. For $\Lambda_c^+ \rightarrow \Sigma^0 K^+ \pi^0$, the violet histograms are the signal MC samples normalized with a product BF of 1.2×10^{-3} [6], the argus function includes seven sub-argus functions. The black point with the error bar is data, the blue solid line represents the total fit function, the gray dashed line shows the combinatorial background, the violet dash line is the signal function, the navy blue dashed line is the un-matched component, cyan dashed line is the background shape extract from $\Lambda_c^+ \rightarrow \Lambda K^{*+}$ MC samples, and red dashed line is the background shape extract from $\Lambda_c^+ \rightarrow \Xi^0 K^+$ MC samples.

$\psi(3686) \rightarrow J/\psi \pi^0 \pi^0$ and $e^+ e^- \rightarrow \omega \pi^0$. The associated systematic uncertainty is assigned to be 3.1% for each π^0 .

- (c) Λ reconstruction: The systematic uncertainty of Λ reconstruction is assigned to be 2.5% by referring to the study of $\Lambda_c^+ \rightarrow \Lambda \pi^+$ in Ref. [34], which includes the systematics associated with reconstructing the daughter particles proton and pion.
- (d) Photon reconstruction: The systematic uncertainty due to the photon reconstruction is estimated to be 0.5% for photon by analyzing the ISR process $e^+ e^- \rightarrow \gamma \mu^+ \mu^-$.
- (e) ΔE requirements: Potential differences in the ΔE distributions between data and MC simulation are studied with the control samples of $\Lambda_c^+ \rightarrow \Sigma^0 \pi^+ \pi^0$ and $\Lambda_c^+ \rightarrow \Sigma^0 \pi^+ \pi^+ \pi^-$. The differences between the nominal and alternative acceptance efficiencies, 2.0% and 3.7%, are taken as the systematic uncertainties for $\Lambda_c^+ \rightarrow \Sigma^0 K^+ \pi^0$ and $\Lambda_c^+ \rightarrow \Sigma^0 K^+ \pi^+ \pi^-$, respectively.
- (f) MC model: The systematic uncertainties associated with the MC model are evaluated with alternative signal MC samples for $\Lambda_c^+ \rightarrow \Sigma^0 K^+ \pi^0$ and $\Lambda_c^+ \rightarrow \Sigma^0 K^+ \pi^+ \pi^-$. These samples are generated as $\Lambda_c^+ \rightarrow \Lambda(1405) K^+$, with $\Lambda(1405) \rightarrow \Sigma^0 \pi^0$ via the PHSP model, and $\Lambda_c^+ \rightarrow \Sigma^0 \pi^+ K^*$, with $K^* \rightarrow K^+ \pi^-$ also simulated in the PHSP model. The differences between the efficiencies of these alternative models and the nominal model are taken as the systematic uncertainties, which are 5.5% for $\Lambda_c^+ \rightarrow \Sigma^0 K^+ \pi^0$ and 18.5% for $\Lambda_c^+ \rightarrow \Sigma^0 K^+ \pi^+ \pi^-$, respectively.
- (g) $\mathcal{B}^{\text{inter}}$: The BFs of $\Sigma^0 \rightarrow \Lambda \gamma$, $\Lambda \rightarrow p \pi^-$ and $\pi^0 \rightarrow \gamma \gamma$, are quoted from the PDG [2]. The uncertainties of these known BFs add up to a total uncertainty of 0.8%.
- (h) Truth matching: To estimate the uncertainty caused by the angle cut in deriving the signal MC shape, we loosen the cut by 5° for each angle. The differences between the nominal and new efficiencies are taken as the systematic uncertainties, which are 5.5% for $\Lambda_c^+ \rightarrow \Sigma^0 K^+ \pi^0$ and 4.9% for $\Lambda_c^+ \rightarrow \Sigma^0 K^+ \pi^+ \pi^-$.
- (i) $N_{\Lambda_c^+ \bar{\Lambda}_c^-}$: The uncertainty of $N_{\Lambda_c^+ \bar{\Lambda}_c^-}$ is quoted from Refs. [12, 14]. Its effect on the BF measurement, 0.9%, is assigned as the systematic uncertainty for both decays.
- (j) MC statistics: The uncertainties due to limited MC statistics are 0.5% for $\Lambda_c^+ \rightarrow \Sigma^0 K^+ \pi^0$ and 0.3% for $\Lambda_c^+ \rightarrow \Sigma^0 K^+ \pi^+ \pi^-$.
- (k) ΔE_Λ requirement: The uncertainty due to the ΔE_Λ requirement is estimated with the control samples of $\Lambda_c^+ \rightarrow \Sigma^0 \pi^+ \pi^0$ and $\Lambda_c^+ \rightarrow \Sigma^0 \pi^+ \pi^+ \pi^-$. The maximum changes of the acceptance efficiencies between data and MC simulation by

varying the ΔE_Λ requirement by ± 0.05 GeV are taken as the systematic uncertainties, which are 0.4% and 0.3% for $\Lambda_c^+ \rightarrow \Sigma^0 K^+ \pi^0$ and $\Lambda_c^+ \rightarrow \Sigma^0 K^+ \pi^+ \pi^-$, respectively.

- (1) $\theta_{\bar{p}\gamma}$ requirement: The systematic uncertainty from the $\theta_{\bar{p}\gamma}$ requirement for $\Lambda_c^+ \rightarrow \Sigma^0 K^+ \pi^0$ is estimated with the control sample of $\Lambda_c^+ \rightarrow \Sigma^0 \pi^+ \pi^0$. The maximum change of the acceptance efficiencies between data and MC simulation after varying the $\theta_{\bar{p}\gamma}$ requirement by $\pm 5^\circ$, 0.1%, is assigned as the systematic uncertainty.

5 Results

The fit result is consistent with a background-only hypothesis of $\Lambda_c^+ \rightarrow \Sigma^0 K^+ \pi^0$ and $\Lambda_c^+ \rightarrow \Sigma^0 K^+ \pi^+ \pi^-$, and the upper limits on their BFs are determined. The distributions of raw likelihoods versus individual BFs are shown as the blue dashed curves in Fig. 4. Each curve is then convolved with a Gaussian function with zero mean and width set as the corresponding multiplicative systematic uncertainty, according to Refs. [35, 36]. The updated likelihood distributions are shown as the red solid lines in Fig. 4. By integrating the red solid curves from zero to 90% of the physical region, the upper limits on the BFs at the 90% C.L. are set to be

$$\begin{aligned} \mathcal{B}(\Lambda_c^+ \rightarrow \Sigma^0 K^+ \pi^0) &< 5.0 \times 10^{-4}, \\ \mathcal{B}(\Lambda_c^+ \rightarrow \Sigma^0 K^+ \pi^+ \pi^-) &< 6.5 \times 10^{-4}. \end{aligned}$$

6 Summary

Based on 4.5 fb^{-1} of e^+e^- annihilation data collected at c.m. energies between 4599.53 MeV and 4698.82 MeV with the BESIII detector at the BEPCII collider, we present the studies of the singly Cabibbo-suppressed hadronic decays $\Lambda_c^+ \rightarrow \Sigma^0 K^+ \pi^0$ and $\Lambda_c^+ \rightarrow \Sigma^0 K^+ \pi^+ \pi^-$ using a single-tag method. The upper limits on their BFs at the 90% C.L. are set to be 5.0×10^{-4} for $\Lambda_c^+ \rightarrow \Sigma^0 K^+ \pi^0$ and 6.5×10^{-4} for $\Lambda_c^+ \rightarrow \Sigma^0 K^+ \pi^+ \pi^-$. The upper limit of the BF of $\Lambda_c^+ \rightarrow \Sigma^0 K^+ \pi^0$ is more stringent than the previous BESIII measurement using a double-tag method [10]. The upper limit of the BF of $\Lambda_c^+ \rightarrow \Sigma^0 K^+ \pi^0$ is

compatible with the theoretical predictions[7, 8] and could not rule out any of them, as shown in Table 4. For $\Lambda_c^+ \rightarrow \Sigma^0 K^+ \pi^+ \pi^-$, the upper limit is less stringent than the BaBar result [11]. These results provide valuable information for understanding the dynamics of charmed baryon decays and improving theoretical models. The sensitivities to these two decays could be further improved with a larger data sample at BESIII [37] in the near future.

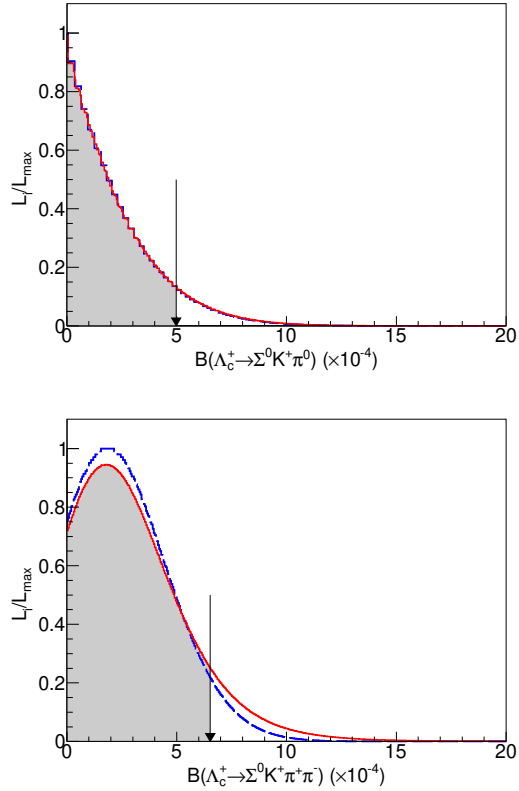


Figure 4. The distributions of the likelihoods versus the BF of $\Lambda_c^+ \rightarrow \Sigma^0 K^+ \pi^0$ (top) and $\Lambda_c^+ \rightarrow \Sigma^0 K^+ \pi^+ \pi^-$ (bottom). The results obtained with and without incorporating the systematic uncertainties are shown in the red solid and blue dashed curves, respectively. The black arrows shows the results corresponding to the 90% C.L..

The BESIII collaboration thanks the staff of BEPCII and the IHEP computing center for their strong support.

References

- G. S. Abrams *et al.*, Phys. Rev. Lett **44**, 10 (1980).
- S. Navas *et al.* (Particle Data Group), Phys. Rev. D **110** (2024) 030001.
- H. B. Li and X. R. Lyu, Natl. Sci. Rev. **8** (2021).
- M. Bauer, B. Stech, and M. Wirbel, Z. Phys. C **34** 103 (1987); Q. P. Xu and A. N. Kamal, Phys. Rev. D **46**, 270 (1992).
- Y. Cheng, Z. Phys. C **29**, 127 (1985).

Table 4. Comparison of the experimental measurements of $\Lambda_c^+ \rightarrow \Sigma^0 K^+ \pi^0$ and $\Lambda_c^+ \rightarrow \Sigma^0 K^+ \pi^+ \pi^-$ obtained in this work, and those of BaBar and BESIII (single-tag) as well as theoretical predictions.

Decay mode	$\Lambda_c^+ \rightarrow \Sigma^0 K^+ \pi^0$	$\Lambda_c^+ \rightarrow \Sigma^0 K^+ \pi^+ \pi^-$
C.Q.Geng <i>et al.</i> [6]	$(1.2 \pm 0.3) \times 10^{-3}$	-
J.Y.Cen <i>et al.</i> [7]	$(0.8 \pm 0.2) \times 10^{-3}$	-
C.Q.Geng <i>et al.</i> [8]	$(8.2 \pm 1.4) \times 10^{-4}$	-
M.Gronau <i>et al.</i> [9]	$(2.1 \pm 0.6) \times 10^{-3}$	-
BESIII (double-tag) [10]	$< 1.8 \times 10^{-3}$	-
BaBar experiment [11]	-	$< 2.5 \times 10^{-4}$
BESIII (single-tag)	$< 5.0 \times 10^{-4}$	$< 6.5 \times 10^{-4}$

- 6 C. Q. Geng, Y. K. Hsiao, C. W. Liu, and T. H. Tsai, Phys. Rev. D **99**, 073003 (2019).
7 J. Y. Cen, C. Q. Geng, C. W. Liu, and T. H. Tsai, Eur. Phys. J. C **79**, 946 (2019).
8 C. Q. Geng, C. W. Liu, and S. L. L, Phys. Rev. D **109**, 093002 (2024).
9 M. Gronau, J. L. Rosner, and C. G. Wohl, Phys. Rev. D **98**, 073003 (2018).
10 M. Ablikim *et al.* (BESIII Collaboration), Phys. Rev. D **109**, 052001 (2024).
11 B. Aubert *et al.* (BaBar Collaboration), Phys. Rev. D **75**, 052002 (2007).
12 M. Ablikim *et al.* (BESIII Collaboration), Chin. Phys. C **46**, 113003 (2023).
13 M. Ablikim *et al.* (BESIII Collaboration), Chin. Phys. C **40**, 063001 (2016).
14 M. Ablikim *et al.* (BESIII Collaboration), Chin. Phys. C **46**, 113002 (2022).
15 M. Ablikim *et al.* (BESIII Collaboration), Nucl. Instrum. Meth. A **614**, 4345 (2010).
16 C. H. Yu *et al.*, Proceedings of IPAC2016, Busan, Korea (2016).
17 X. Li *et al.*, Radiat. Detect. Technol. Methods **1**, 13 (2017).
18 Y. X. Guo *et al.*, Radiat. Detect. Technol. Methods **1**, 15 (2017).
19 P. Cao *et al.*, Nucl. Instrum. Meth. A **953**, 163053 (2020).
20 M. Ablikim *et al.* (BESIII Collaboration), Chin. Phys. C **44**, 040001 (2020).
21 S. Agostinelli *et al.* (GEANT4 Collaboration), Nucl. Instrum. Meth. A **506**, 250 (2003).
22 S. Jadach, B. F. L. Ward, and Z. Was, Phys. Rev. D **63**, 113009 (2001).
23 M. Ablikim *et al.* (BESIII Collaboration), Phys. Rev. Lett. **131**, 191901 (2023).
24 D. J. Lange, Nucl. Instrum. Meth. A **462**, 152 (2001).
25 R. G. Ping, Chin. Phys. C **32**, 599 (2008).
26 C. Chen, G. S. Huang, X. R. Qi, D. H. Zhang, and R. G. Ping, Phys. Rev. D **62**, 034003 (2000).
27 X. Yang, R. G. Ping and H. Chen, Chin. Phys. Lett. **31**, 052001 (2008).
28 H. Albrecht *et al.* (ARGUS Collaboration), Phys. Lett. B **303**, 163 (1993).
29 M. Punzi, arXiv:physics/0308063.
30 H. Albrecht *et al.* (ARGUS Collaboration), Phys. Lett. B **241**, 278-282 (1990).
31 M. Ablikim *et al.* (BESIII Collaboration), Phys. Rev. D **99**, 112005 (2019).
32 M. Ablikim *et al.* (BESIII Collaboration), Phys. Rev. Lett. **116**, 052001 (2016).
33 K. Stenson, arXiv:physics/0605236.
34 X. X. Liu, X. R. Lyu, and Y. S. Zhu, Chin. Phys. C **39**, 113001 (2015).
35 M. Ablikim *et al.* (BESIII Collaboration), Chin. Phys. C **44**, 040001 (2020).